Direct-Digital Phase-Noise Measurement

J. Grove, J. Hein, J. Retta, P. Schweiger, W. Solbrig, and S.R. Stein
Timing Solutions Corporation
Boulder, Colorado
srstein@timing.com

Abstract— **We have completed a Phase 1 SBIR project to develop technology for direct phase-noise measurements. This new approach to phase-noise measurements uses fast analog-to-digital converters to digitize the input RF signal and performs all down-conversion and phase detection functions by digital signal processing. It has several significant advantages over analog phase-noise measurement techniques: There is no external phase-lock loop, oscillators can be compared at different frequencies, amplitude and phase noise may be measured simultaneously, the spectrum and Allan variance may be computed simultaneously, and complex calibration techniques are eliminated.**

Keywords-phase noise; analog-to-digital converter; digital signal processing; phase detector.

I. INTRODUCTION

Traditionally, phase noise measurements are made by analog techniques [1]. The phase fluctuations are transduced to a voltage that is sampled and Fourier analyzed. The transducer is almost always a double-balanced mixer that, along with the following low noise amplifiers, must be calibrated at all Fourier frequencies of interest. The double balanced mixer operates as a phase detector only when the signals at the local oscillator and signal ports are approximately in phase quadrature. Thus analog phase noise measurements of two sources require that the unit under test be phase locked to the reference. By using digital techniques, it is possible to eliminate both of these restrictions making it much simpler to make high quality phase noise measurements. Figure 1 shows the analog approach to source phase noise measurements.

The digital method samples the RF waveforms rather than the output of the phase detector [2]. The phase detection is performed by digital signal processing, which results in several advantages: the phase detector has $2N\pi$ range eliminating the need for a phase-lock loop and all digital filters are sufficiently flat to eliminate the need to calibrate individual measurements. It is possible to make the signal processing errors fall below the noise of the analog-to-digital converters, which then determine the noise floor of the direct-digital phase-noise measurement system. As will be seen below, this noise is rather high, but can be reduced to useful levels through the application of cross correlation [3]. The concept for direct-digital phase-noise measurements is shown in Figure 2.

Funded in part by NIST under Order No. SB1341-03-W-0817

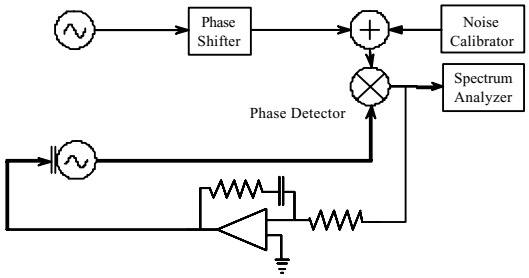

Figure 1: Analog source phase-noise measurements require both calibration and a phase-lock loop

The project consisted of two parts. In the first part (Phase 1 SBIR), we constructed a prototype phase detector coupled to a fast PCI-X server to collect the data. Batch data analysis, performed using Matlab, allowed us to determine the wideband noise floor and the flicker noise of the ADCs. The hardware was operated over the input frequency range of 1 to 30 MHz and three ADCs from different manufacturers were evaluated. We found consistent wideband noise levels of approximately -150 dBc/Hz from the ADC electronics and flicker levels of -145 dBc/Hz at a 1 Hz frequency offset from a 5-MHz carrier. The ADC quantization noise was always less than the circuit noise. Using cross correlation, we achieved 5-MHz noise floors of -155 dBc/Hz at 1 Hz and -170 dBc/Hz broadband.

The first part of the project identified several difficult technical issues with the direct measurement approach. The first is the 29 ps/C temperature coefficient of the ADCs,

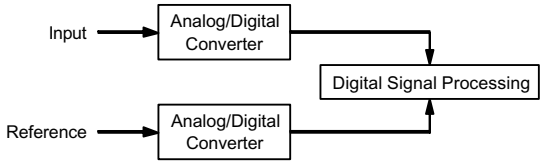

Figure 2: The RF signals are immediately converted to digital samples in order to perform direct-digital phase-noise measurements.

which can increase the low-frequency noise above the flicker noise level. The second is the high speed processing required to perform the FFT computations in real time. These challenges had to be overcome in order to build a practical instrument using this technique.

In the second part of the project, after the conclusion of the Phase 1 SBIR, we constructed prototype hardware to perform the direct-digital phase-noise measurements in real time. This provided the opportunity to both address the thermal issues and assess the hardware necessary to perform all the needed processing in practical FPGA and DSP chips.

II. THEORY

All the analog-to-digital converters evaluated in this study had 14 to 15 bits of precision and maximum sampling rates of 75 to 105 MHz. In order to prevent harmonics, spurs, and noise from aliasing into the measured spectrum, a 30-MHz analog anti-alias filter was employed before the RF signals were sampled. The heart of the approach is the down converter that immediately follows the sampler. In-phase samples of each input signal are multiplied by the sine and cosine of a synthesized local oscillator and low-pass filtered. When the LO frequency is approximately equal to the input frequency the output of the filters are in-phase (I) and quadrature (Q) base-band samples. The phase difference between the input signal and the synthesized LO is computed using the arctangent function as shown in Figure 3.

This step is the heart of the direct-digital technique. It is not necessary to down-convert to DC before computing the phase difference. A small DC offset causes the phase to accumulate nearly linearly. Although the arctangent function is restricted to values between $-\pi$ and $+\pi$, it is possible to un-wrap the phase and recover the correct linear function. This should be contrasted with the analog approach. The double balanced mixer produces a distorted sine function of the phase difference. As the two inputs approach the in-phase condition, the output of the mixer is insensitive to the phase difference between the signals and the distortion makes it impossible to accurately compute the phase even if quadrature mixers were employed. Thus analog test sets must be maintained near quadrature where the sine of the phase is nearly linear and equal to the phase angle. When measuring sources, the quadrature condition is achieved by a long time constant phase-lock loop.

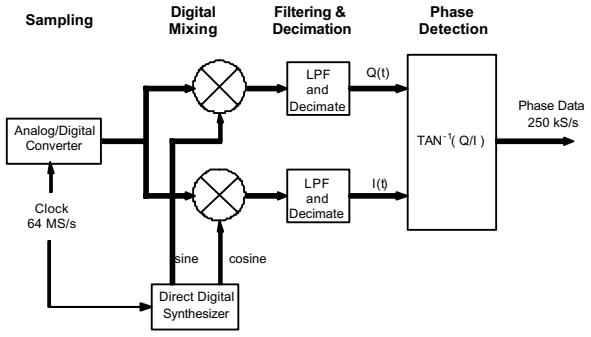

Figure 3: A local oscillator synthesized from the internal clock down-converts the input to base-band where the samples are used to compute the phase difference between the LO and the input.

Down-conversion is performed on the second input channel and then the two are subtracted to obtain the phase difference between the two sources. However, if the two input signals have different nominal frequencies, then the phase of the second channel must be scaled to the same nominal frequency as the first channel. For example if we were calculating the phase difference between a 10-MHz signal and a 5-MHz signal, then the phase difference between the 5-MHz source and the LO must be multiplied by 2 before subtraction from the phase difference of the 10-MHz signal and its LO. The subtraction process causes the phase noise of the instrument's clock oscillator to cancel just as it does in a dual-mixer phase-difference measurement system.

The frequency content of the measured phase difference is analyzed by computing the Discrete Fourier Transform (DFT) of the phase difference. The computation to this point is shown in Figure 4. However, if the Power Spectral Density (PSD) of the phase were computed from the DFT the broadband noise floor would be limited by the white noise of the ADCs at a level of -150 dBc/Hz or worse with today's best converters. This is the price that has been paid for the convenience of operation without a PLL or need for calibration and would make the direct-digital approach uninteresting for measuring precision oscillators except for the fact that convenient methods exist to overcome the limitation.

Instead of computing the magnitude-squared of the DFT to obtain an estimate of the PSD, we compute the cross spectrum of two identical measurement systems as shown in Figure 5. The ADC noise is highly uncorrelated and averages down, allowing improvement of the broadband noise floor to better than -170dBc/Hz.

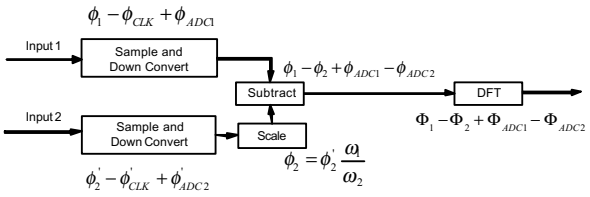

Figure 4: After down-conversion, the phase differences are scaled, subtracted, and Fourier analyzed to determine the frequency content

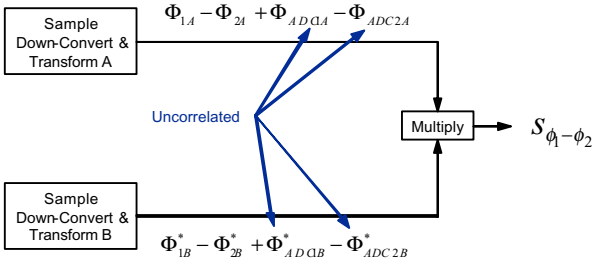

Figure 5: The PSD is computed as the cross-spectrum of the DFTs from two identical processing front ends

Finally, in order to produce a useful PSD estimate the spectrum estimation process is broken into a series of spans that have appropriate frequency resolution (DFT length). The process is shown in figure 6. This process allows more rapid estimation of the higher frequency portions of the spectrum. Data for each lower frequency span is obtained by low-pass (anti-alias) filtering the higher sample rate data and then decimating it appropriately.

III. PERFORMANCE

A. *Part 1 of the Project*

During the first part of this project blocks of data were acquired from commercial ADCs operating at 96 or 100 M sample/s. The samples were down-converted using a Gray-chip tuner and then filtered, decimated, and stored on a fast PCI-X computer. A large RAID array allowed several days of data to be acquired and stored for subsequent processing. Figure 7 illustrates most of the important things that were learned during this part of the project.

Above 100 Hz, the measured phase noise of the individual measurement sections is limited by the white noise of the ADCs to a value between -140 dBc/Hz and -150 dBc/Hz. The precise level depends on the ADC and the input signal level. The third and lower curve is the cross spectrum. The fact that the cross spectrum lies below the measurement section spectra demonstrates that the ADC noise is uncorrelated to some degree. We expected flicker noise to dominate the spectrum below 100 Hz, but instead observed that the slope was f^{-2}. However, by taking data for a very long time we were able to show that the f^{-2} slope did not continue forever, but peaked at a Fourier frequency corresponding to a 22 minute period. We concluded that the low frequency behavior was dominated by the temperature coefficient of the ADCs. Data such as those in Figure 7 encouraged us to proceed to design custom hardware to perform direct-digital phase-noise measurements in real time.

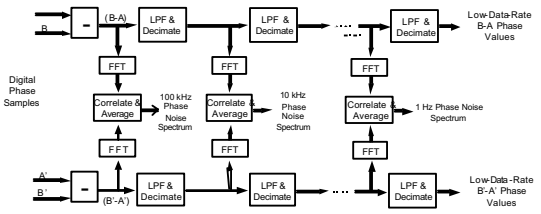

Figure 6: Successive Filter-Decimate-Transform Signal Processing Stages

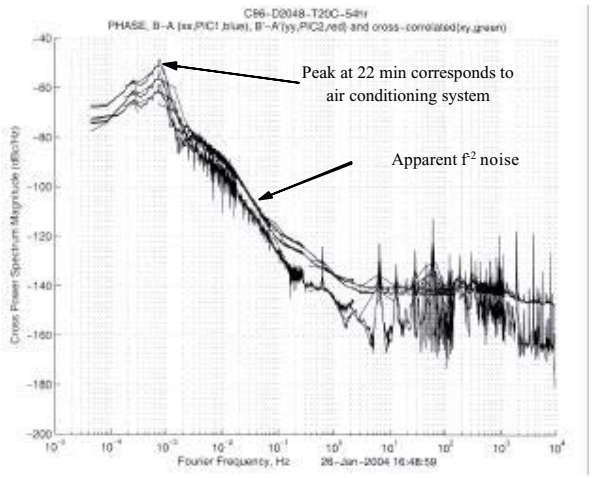

Figure 7: Individual PSD estimates from Part 1 of the project and the cross-spectrum PSD estimate

B. *Part 2 of the Project*

Hardware was designed specifically to perform the direct-digital phase-noise measurements in real time. Particular attention was paid to

- Stabilizing the temperature of the ADCs
- Reducing correlated noises such as the internal clock noise
- Performing all computations with sufficient bits to preserve the instrument noise floor
- Apportioning the computation between the FPGAs and DSPs so that it runs in real time

The second part of the project exceeded our expectations and the remaining figures illustrate the performance that has been obtained. The hardware was built into a prototype instrument with VGA display. Software was written to control all the functions. The entire measurement process is controlled with two buttons: start and stop, while soft keys allow the user to configure the display. Figure 8 shows the prototype instrument, which operates over the frequency range of 1-30 MHz.

A calibration was performed using a calibrated noise source, which adds -106.6±0.2 dBc/Hz/dBm noise to a 12.3±0.5 dBm carrier. Thus the calibrated phase-noise input is -118.9±0.5 dBc/Hz. The measured value shown in Figure 9 was -118.7 dBc/Hz, which is well within the 1 σ error limits. The ±0.2 dB variations of the measured phase noise around the mean are probably indicative of the potential accuracy of the direct-digital phase-noise measurement technique.

Figure 8: Prototype instrument

Figure 10 shows the noise floor of the direct-digital approach at 10 MHz. It was measured by driving both inputs of the test set with 10 MHz from a 3-dB splitter. The flicker phase level is -145 dBc/Hz at a 1 Hz offset frequency and the broadband noise is about -173 dBc/Hz for offsets greater than 1 kHz from the carrier. A number of spurs are evident in this and other plots. Empirical tests indicate that some of the spurs are the result of finite word lengths in the FPGAs and DSPs. Simulation analysis indicates that other spurs result from DC offsets in the mixing process. We believe that they will be reduced below the noise by future improvements in processing such as pseudorandom noise modulation to spread their power and cause it to de-correlate.

The final three plots show some of the power of the direct-digital phase-noise measurement technique. Figure 11 illustrates that the direct-digital technique can be used to

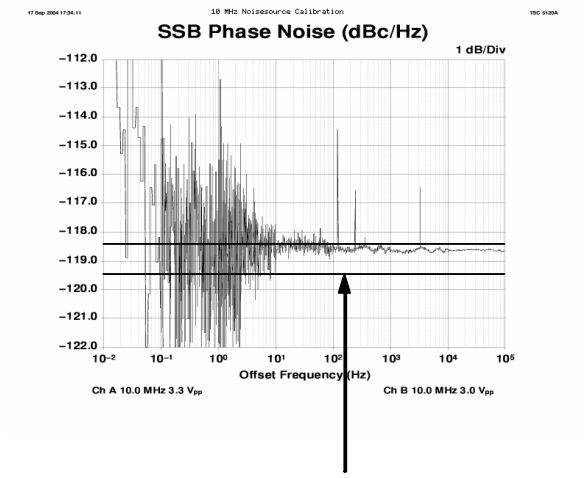

Calibrated phase noise source with value of –118.9±0.5 dBc/Hz

Figure 9: Comparison of direct phase-noise measurements with a calibrated noise source

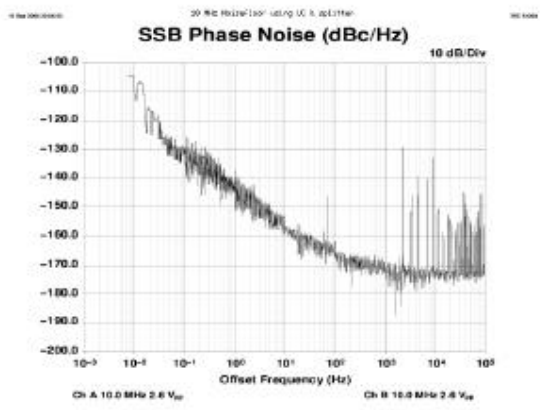

Figure 10: 10-MHz noise floor of the prototype instrument

make measurements on two-port devices. The signal from a low-noise source was split and each arm was connected to a distribution amplifier and then to the measurement system. The measurements were made without any need to set the phase relationship between the two inputs. It is quite evident that the broadband noise has settled to a value with excellent precision. This characteristic is observed whenever there are enough averages for cross correlation to reduce the noise floor sufficiently below the noise being measured. The value at 1-Hz offset has considerably lower precision since the measured noise is within 5 dB of the noise floor and there are significantly fewer averages.

Figure 12 depicts the phase noise of an Agilent 83732B Synthesizer at 11.123456 MHz compared to a very low-noise 10-MHz reference. It demonstrates that the direct-digital technique is indeed capable of making phase-noise measurements at arbitrary frequencies within its 1-30 MHz operating range. The measured synthesizer noise agrees well with the published specifications. Finally, Figure 13 shows the combined phase noise of two low-noise quartz oscillators. The frequency of one oscillator was at approximately 5 MHz and the other was 8.5 Hz lower in frequency. Despite the 8.5 Hz frequency offset, the direct-digital technique is able to make the phase-noise measurement.

IV. CONCLUSIONS

We have used direct-digital techniques to make extremely sensitive phase-noise measurements, comparable to the best available commercial analog instruments. The RF signals are directly converted to high-speed digital samples and all further processing is performed numerically. Two great advantages accrue as a result. The first is that it is unnecessary to maintain the signal and reference in a fixed phase relationship or even at the same frequency. As a result, the phase noise of two oscillators may be measured without the use of a phase-lock loop. The second advantage is that the technique yields measurements accurate to better than 1 dB without the traditional calibration of phase detector and

low-noise amplifiers. These two features make it possible to construct a totally automatic phase-noise measurement instrument that performs the entire task at the press of a single button.

REFERENCES

[1] D. A. Howe, D. W. Allan, and J. A. Barnes, "Properties of Signal Sources andMeasurement Methods," Proceedings of the 35th Annual Frequency Control Symposium, 1981, pp A1-A47.

[2] G. Paul Landis, Ivan Galysh, and Thomas Petsopolous, "A new Digital Phase Measurement System," Proceedings of the 33rd Annual Precise Time and Time Interval Meeting, 2001, pp 543-552.

[3] F. L. Walls, S. R. Stein, James E. Gray, and David J. Glaze, "Design Considerations in State-of-the-Art Signal Processing and Phase Noise Measurement Systems," Proceedings of the 30th Annual Frequency Control Symposium, 1976, pp 269-274.

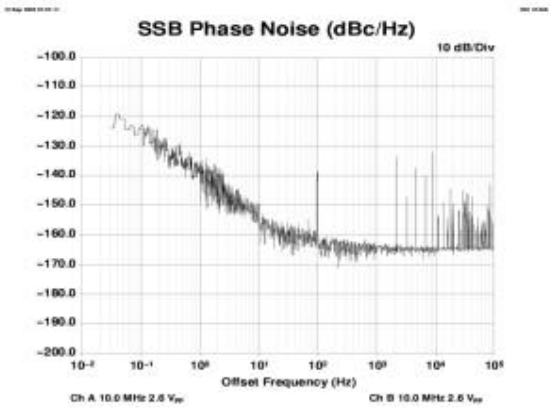

Figure 11: Measurement of a pair of TSC 2036C distribution amplifiers at 10 MHz

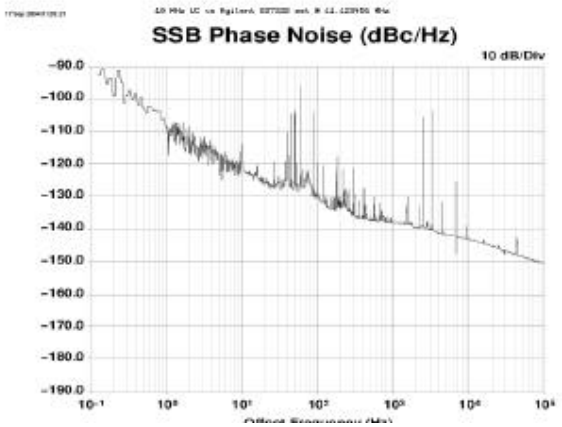

Figure 12: An Agilent 83732B Synthesizer at 11.123456 MHz vs. a 10-MHz reference

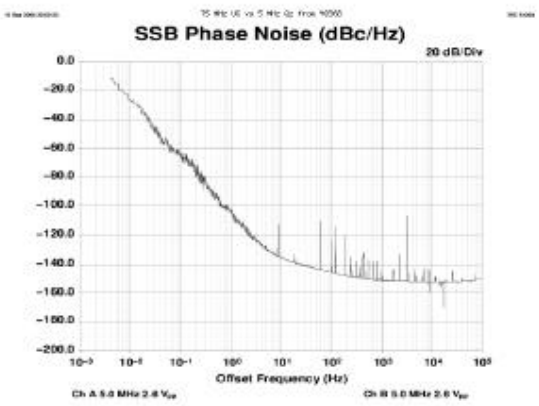

Figure 13: Comparison of two 5-MHz sources separated by 8.5 Hz